

Averaging Effects in PGSE NMR Attenuations Observed in Bimodal Molecular Weight PMMA Solutions

Scott A. Willis, Gary R. Dennis, Gang Zheng, and William S. Price*

Nanoscale Organisation and Dynamics Group, College of Health and Science, University of Western Sydney, Locked Bag 1797, Penrith South DC, NSW 1797, Australia

Received July 28, 2010

ABSTRACT: NMR diffusion measurements have proven to be a very powerful technique for probing the solution dynamics of polymer systems. In theory, it is possible to extract a range of useful information including molecular weights from the diffusion data. In practice, especially outside the infinite dilution regime, the data analysis is further complicated by numerous effects including macroscopic and microscopic averaging. Here the averaging effects in dilute bimodal narrow molecular weight poly(methyl methacrylate) in deuterated chloroform solutions are studied at 298 K and cogent models developed to analyze the data. Simulations are performed which represent different limits of diffusive behavior in bimodal solutions and the suitability of the simulations are found to be dependent on the ratio of the molecular weights in the solution.

Introduction

Translational diffusion studies can provide immense amounts of information about the solution properties of molecules. Self-diffusion does not require a chemical potential gradient,¹ and is a result of internal kinetic energy.² Diffusion is related to molecular size through the Stokes–Einstein–Sutherland equation which relates the diffusion of a particle to its hydrodynamic size^{2–4} and solution viscosity,⁵ and is sensitive to molecular interactions.⁶ For a freely diffusing species it can provide an estimate of the mean square displacement of a molecule whereas for restricted diffusion it can give the size of the restricting geometry and/or the direction dependent apparent diffusion coefficients if the system is anisotropic.² Self-diffusion measurements can be conveniently made with pulsed gradient spin–echo (PGSE) NMR.^{2,3,7,8}

In an NMR diffusion measurement of a freely diffusing monodisperse sample the echo decay is monoexponential since there is only one diffusion coefficient. However, in a polydisperse polymer solution there must be a range of diffusion coefficients and the components generally have overlapped NMR signals.⁹ Macroscopic and microscopic averaging of the diffusion coefficients are often observed for polydisperse macromolecular systems.^{3,10} Phenomena such as obstruction and entanglement, which are both dependent on concentration, may influence the diffusion coefficients since these effects occur on smaller time scales and would be averaged for the diffusion measurement time scale; i.e., the average molecular spacing is less than the mean square displacement on the experimental time scale and as such molecules will collide and interact.^{2,3}

Exploring the effects of polydispersity on NMR diffusion measurements is of great significance. In this work, the diffusional averaging effects in dilute bimodal mixtures of poly(methyl methacrylate) (PMMA) in deuterated chloroform were studied at 298 K and at concentrations less than the overlap concentration, $c < c^*$, and compared to the diffusion coefficients in monomodal solutions.

Theoretical Basis

PGSE NMR. PGSE NMR may be used to measure the diffusion of molecules by using the Larmor frequency as a

label for position.² Using the simplest PGSE NMR sequence: the Stejskal and Tanner sequence (a modified Hahn spin–echo),¹¹ as an example, the echo signal and echo attenuation for a single freely diffusing species is given by³

$$S(g, t_{aq}) = S(0, t_{aq})E(g, \Delta) \quad (1)$$

where

$$E(g, \Delta) = \frac{S(g, t_{aq})}{S(0, t_{aq})} = \exp\left(-\gamma^2 g^2 D \delta^2 \left(\Delta - \frac{\delta}{3}\right)\right) \\ = \exp(-bD) \quad (2)$$

respectively, where $S(g, t_{aq})$ is the total signal observed with gradient strength $g \text{ T m}^{-1}$, $S(0, t_{aq})$ is the signal when the gradient strength is 0 T m^{-1} , $E(g, \Delta)$ gives the signal (normalized) with attenuation from diffusion, δ is the duration of the gradient pulse in seconds, γ is the gyromagnetic ratio of the nucleus, Δ is the diffusion time in seconds, and t_{aq} is the time of acquisition. As shown in eq 2, all of the magnetic gradient parameters can be lumped into the b factor. The diffusion coefficient, $D \text{ (m}^2 \text{ s}^{-1}\text{)}$, can be obtained by nonlinear regression of eq 2. Other experimental considerations can be found elsewhere.^{3,12–15}

PGSE NMR of Polydisperse Systems. In a polydisperse system, obstruction of the smaller molecules by the larger ones causes a reduction in their diffusion coefficient.³ Modeling such obstruction effects is complex due to the shape of the molecules and their distribution in solution and in concentrated solutions the modeling of obstruction becomes a complex many body problem.¹⁶ The available models are simplistic as they assume that the obstruction is due to evenly distributed monodisperse hard spheres.^{3,7} The situation becomes further complicated when the small molecules bind to the surface of the larger ones.³ Self-obstruction reduces the diffusion coefficient of the molecules as well, and models may overestimate the reduction as the concentration increases since they may not include aggregation effects.^{3,17,18}

Macroscopic and microscopic averaging are often observed for polydisperse systems. The macroscopic average

*Corresponding author. E-mail: w.price@uws.edu.au.

describes how the attenuation can be described by averaging each of the component diffusion coefficients scaled by their concentrations in the polydisperse system.¹⁰ The logarithmic attenuation plots for polymers should be noticeably nonlinear for polydispersities above 1.06.^{10,19} However, the attenuation curves from diffusion in polydisperse systems often do not show the expected functional dependence. This was observed for a polydisperse dextran solution²⁰ and a lysozyme solution where aggregation was known to occur.¹⁷ The deviation from the expected macroscopic average is known as microscopic averaging or ensemble averaging.^{3,10,20} The distribution of diffusion coefficients measured in the polydisperse system is narrower than expected.^{3,10,21} The averaging process may also depend on concentration which suggests it is a result of molecular interactions (polymer–polymer and/or polymer–solvent).^{10,19,20} Thus, the measured attenuation plots include both macroscopic and microscopic averaging.¹⁰

At infinite dilution the diffusion of each component is unperturbed by the presence of the others, and so the microscopic averaging disappears and only macroscopic averaging applies.^{19,22} Bimodal mixtures of two nearly monodisperse polymers have been studied to demonstrate the averaging processes.^{10,22,23} Deuterated polymers may be used so that one component is “NMR invisible”.^{10,22,23} Comparison is often made between the diffusion coefficients of the components in the mixture and those of each component polymer however this is sometimes only done for the same total polymer concentrations¹⁰ and not the same component concentrations. It has been noted that the measured diffusion coefficient of the smaller molecule decreases while that of the larger molecule increases when measured in a bimodal solution.^{10,19}

General Case. The PGSE NMR attenuation of a sample consisting of a discrete mixture can be described by a summation of the contributing decays.^{3,10,17,19,20,22,24} Generally,

$$S(g, t_{aq}) = \sum_i S_i(0, t_{aq}) E_i(g, \Delta) \quad (3)$$

and

$$S(g, t_{aq}) = \sum_i M_i n_i \exp(R_i) \exp(-bD_i) \quad (4)$$

where M_i , n_i , and R_i are the molecular weight, number of moles, and the spin relaxation term for component i , respectively.

If the relaxation term is assumed to be identical for all resonances irrespective of M_i , as considered for simplicity to allow for normalization,^{3,10,17,19,20} eq 4 becomes

$$\begin{aligned} \ln(E(g, \Delta)) &= \ln \left(\frac{\sum_i M_i n_i \exp(-bD_i)}{\sum_i M_i n_i} \right) \\ &= -b \left(\frac{\sum_i M_i n_i D_i}{\sum_i M_i n_i} \right) \end{aligned} \quad (5)$$

Thus, the PGSE NMR experiment measures a weighted average diffusion coefficient,^{3,17,20}

$$\langle D \rangle_w = \frac{\sum_i M_i n_i D_i}{\sum_i M_i n_i} \quad (6)$$

which can then be expressed in terms of the diffusion average molecular weight.^{19,25,26}

To reflect the polydispersity of a system, extra terms can be included in eq 5.^{3,17,20} These arise from noting that eq 5 can be considered a cumulant-generating function,^{3,17,27,28} with the moment-generating function being E , and expansion to the second cumulant gives the variance or width of the distribution of diffusion coefficients about $\langle D \rangle_w$. Equation 5 is the first cumulant.

For a polydisperse system with a continuous distribution of molecular weights, the summations in eq 5 can be replaced by integrals,^{10,19}

$$E(g, \Delta) = \frac{S(g, t_{aq})}{S(0, t_{aq})} = \frac{\int_0^\infty M_i n(M)_i \exp(-bD_i) dM}{\int_0^\infty M_i n(M)_i dM} \quad (7)$$

Since the attenuation equation is a sum of exponentials for a polydisperse system, if the data is plotted on a logarithmic scale then the attenuation curve should be nonlinear.^{3,10,17,20}

However, macroscopic and microscopic averaging may result in the logarithmic attenuation curves appearing different than predicted. Other factors may also affect the deconvolution of superimposed exponential decays. For example, even when there are two different diffusion coefficients present, a simple biexponential fit to the attenuation data is affected by the signal-to-noise ratio, instrumental error, the ratio of the signals of the contributing components, and the ratio of the diffusion coefficients.²⁹ Additionally, the variation of relaxation with M may be negligible only at certain concentrations.^{19,24,30} The effects of obstruction and relaxation need to be considered in both the design and interpretation of PGSE NMR experiments.^{7,17,31}

Bimodal case. From eqs 3 – 7, the PGSE NMR attenuation for a discrete bimodal system is given by

$$E(g, \Delta) = \frac{M_1 n_1 \exp(R_1) \exp(-bD_1) + M_2 n_2 \exp(R_2) \exp(-bD_2)}{M_1 n_1 \exp(R_1) + M_2 n_2 \exp(R_2)} \quad (8)$$

For a bimodal polymer solution of equal weight fractions (i.e., $M_1 n_1 = M_2 n_2$), eq 8 simplifies to

$$E(g, \Delta) = \frac{\exp(R_1) \exp(-bD_1) + \exp(R_2) \exp(-bD_2)}{\exp(R_1) + \exp(R_2)} \quad (9)$$

and if the relaxation terms are independent of the molecular weight (i.e., $R_1 = R_2$) this can be further simplified to

$$E(g, \Delta) = 0.5 \exp(-bD_1) + 0.5 \exp(-bD_2) \quad (10)$$

Experimental Section

Polymers. Narrow molecular weight PMMA samples were obtained from Polymer Laboratories (U.K.) and had the following peak molecular weights, M_p , and polydispersities: 4700 g mol⁻¹ (1.07), 12 700 g mol⁻¹ (1.08), 20 200 g mol⁻¹ (1.06), 68 000 g mol⁻¹ (1.07), and 143 000 g mol⁻¹ (1.04).

Pulsed Gradient Spin-Echo NMR. ¹H NMR diffusion experiments were performed at 298 K with a Bruker Avance 400 MHz with 5 mm broadband X(H)(BBO) probe equipped with a z-axis gradient. All data fitting was performed using OriginPro 8 (OriginLab Corporation, MA) software using the Levenberg–Marquardt algorithm. The temperature was calibrated using a

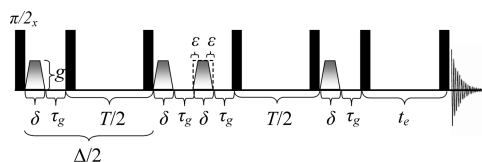


Figure 1. DSTE sequence with trapezoidal gradient pulses and a longitudinal eddy current delay (t_e). This sequence contains two stimulated echo (STE) sequences with the diffusion time in each STE being $\Delta/2$ giving a total diffusion time of Δ . The rise and fall time of the trapezoidal gradient pulses is ε and the total gradient pulse width is δ .

methanol sample.^{32,33} All polymer diffusion measurements were performed with the double stimulated echo (DSTE) pulse sequence with trapezoidal gradient pulses (Figure 1). This sequence was chosen to minimize convection problems and because in macromolecular samples the spin–lattice relaxation time (T_1) is much greater than the spin–spin relaxation time (T_2).¹² The attenuation of the DSTE pulse sequence (derived with trapezoidal gradient pulses using Maple 12 (Maplesoft, Waterloo Maple, Inc.)) and dependence on relaxation (given by Jerschow and Müller³⁴) are given by

$$E(g, \Delta) = \frac{S(g, t_{aq})}{S(0, t_{aq})} = \exp \left\{ - \left[\gamma^2 g^2 \left(\delta^2 \left(\Delta - \frac{2\delta}{3} \right) + B_{\text{trapezoid}} \right) \right] D \right\} \quad (11)$$

where

$$B_{\text{trapezoid}} = \left(-2\delta\varepsilon\Delta + 2\delta^2\varepsilon + \frac{16\varepsilon^3}{15} - \frac{35\delta\varepsilon^2}{15} + \varepsilon^2\Delta \right) \quad (12)$$

and

$$S(0, t_{aq}) \propto \exp \left(- \frac{4(\delta + \tau_g)}{T_2} - \frac{(\Delta - 2\delta - 2\tau_g + t_e)}{T_1} \right) \quad (13)$$

where the delays (Δ , δ , τ_g , T , t_e , ε) (in s) are shown in Figure 1. The data was normalized to the signal at 0.011 T m⁻¹ gradient strength since the signal with 0 T m⁻¹ gradient strength of stimulated echo type sequences can be affected by cosine modulation dependent on chemical shift.^{15,35}

Diffusion Measurements of Monomodal Polymer Solutions. The measured diffusion coefficients of monomodal polymer solutions were assigned to a single molecular weight, i.e., M_p . The diffusion coefficients were measured in monomodal polymer solutions at concentrations equivalent to the total polymer concentration in the bimodal solutions and the correct component concentrations in the bimodal solutions. The required amount of polymer was weighed directly into the NMR tube, 400 μ L of CDCl₃ was added, and the polymer solutions were allowed to equilibrate for at least 3 h, after which the solution was thoroughly mixed. The meniscus was marked to check for solvent evaporation during NMR experiments.

The values of δ , Δ , and g were selected so that the signal attenuated to 10% of the signal without gradient. Typical acquisition parameters were: recycle delay time between diffusion experiments of 28–35 s ($5 \times T_1$ of CHCl₃—which was longer than any of the polymer resonances—so that the diffusion coefficient of CHCl₃ could also be measured), δ ranged from 2 to 8 ms, Δ ranged from 0.07 to 0.65 s, $\varepsilon = 50 \mu$ s, $\tau_g = 200 \mu$ s, $t_e = 5$ ms, a spectral width of 8250 Hz digitized into 8k or 16k data points, g was typically varied from 0.011 to 0.469 T m⁻¹ in increments of 0.029 T m⁻¹ (a total of 17 data points for each

attenuation curve). Each spectrum was averaged over 8 scans. The CHCl₃ signal was integrated over the range 7.20–7.40 ppm, and the CH₂ signal of the PMMA was integrated over the range 1.72–2.61 ppm. The diffusion coefficients were determined from nonlinear regression of eq 11 onto the PGSE NMR data to avoid unequal weighting to noise (as is the case when using the logarithmic form of eq 11 during data fitting). While the errors taken for the diffusion coefficients were the standard errors from the data fitting, it should be noted that after including factors like inherent gradient inhomogeneity and gradient calibration errors one can expect a variation of the order of 1% for duplicate measurements.

Relaxation Measurements of Monomodal Polymer Solutions.

The longitudinal and transverse relaxation was measured for monomodal polymer solutions using the inversion recovery technique^{36,37} and the Carr–Purcell–Meiboom–Gill (CPMG) sequences,^{38,39} respectively. The relaxation was measured for three concentrations (approximately 1.5, 0.75 and 0.31% w/v) for each molecular weight. The dependences of T_1 and T_2 on both molecular weight and concentration were then found.

Diffusion Measurements of Bimodal Polymer Solutions. The attenuation plots and diffusion coefficients were measured in bimodal (50:50 by weight) polymer solutions (total concentration $\sim 1.5\%$ w/v). The bimodal solutions were 4700 g mol⁻¹/143 000 g mol⁻¹ (M_p ratio = 30.4), 12 700 g mol⁻¹/68 000 g mol⁻¹ (M_p ratio = 5.4) and 20 200 g mol⁻¹/68 000 g mol⁻¹ (M_p ratio = 3.4). Two samples of each bimodal mixture were prepared and the diffusion attenuation in each solution was measured twice. The parameters were similar to those used in the monomodal diffusion measurements. The analysis involved comparison of the experimental bimodal attenuation curves to the simulated attenuation curves using the diffusion coefficients measured in the monomodal solutions. Two types of simulations were made: simulation A, the diffusion coefficients used were those measured for the component polymer in a monomodal solution of the same *total* polymer concentration as the bimodal solution (i.e., $\sim 1.5\%$ w/v); simulation B, the diffusion coefficients used were those of the component polymer in a monomodal solution of the same *component* concentration as in the bimodal solution (i.e., $\sim 0.75\%$ w/v). Relaxation terms were included for completeness in the simulations and analysis (i.e., eq 9). For a DSTE with trapezoidal pulses (cf eq 11)

$$b = \left[\gamma^2 g^2 \left(\delta^2 \left(\Delta - \frac{2\delta}{3} \right) + B_{\text{trapezoid}} \right) \right] \quad (14)$$

and $B_{\text{trapezoid}}$ is given by eq 12 as derived in this work. The relaxation terms given by Jerschow and Müller³⁴ but with molecular weight dependence are

$$R_i = \left[- \frac{4(\delta + \tau_g)}{T_2(M_i)} - \frac{(\Delta - 2\delta - 2\tau_g + t_e)}{T_1(M_i)} \right], \quad i = 1 \text{ or } 2 \quad (15)$$

where $T_1(M_i)$, $T_2(M_i)$ indicate that the relaxation is a function of molecular weight.

Results and Discussion

Relaxation in Monomodal Polymer Solutions. The spin–lattice and spin–spin relaxation measurements showed that the relaxation term should be included in the analysis of the diffusion of these polymer systems. The concentration dependence of the longitudinal and spin–spin relaxation, if significant, may be used to find a normalizing function in analyzing the PGSE data.^{40,41} In doing so the effects of the influence of local chain/segment dynamics on the measured diffusion coefficient may be removed.^{40,41} However, the concentration dependence of the relaxation of the PMMA

Table 1. Exponential Values of the Relaxation Terms (eq 15) for Simulations and Fitting of Bimodal Data from the DSTE Experiments

component 1 (g mol ⁻¹)	component 2 (g mol ⁻¹)	M_p ratio	exp(R_1)	exp(R_2)
4700	143 000	30.4	0.410	0.370
12 700	68 000	5.4	0.504	0.493
20 200	68 000	3.4	0.447	0.445

samples was negligible in the concentration range and was ignored.

The molecular weight dependence, however, could be described by a single exponential function:

$$T_1(s) = (0.36 \pm 0.01) - (0.14 \pm 0.05) \exp\left(\frac{-M_p}{(5900 \pm 2700)}\right) \quad (16)$$

$$T_2(s) = (0.048 \pm 0.001) + (0.057 \pm 0.019) \exp\left(\frac{-M_p}{(5500 \pm 1600)}\right) \quad (17)$$

However, even for these narrow molecular weight polymers, some averaging of the different types of protons was evident in the longitudinal and spin–spin relaxation measurements since minor deviations from the expected mono-exponential behavior were observed. Nevertheless, the approximate relaxation times are still valuable when describing the attenuation in these systems. Equations 16 and 17 were used to calculate the relaxation terms (i.e., eq 15) for use with eq 9 for simulations and fitting of the bimodal data (Table 1).

Diffusion in Bimodal Polymer Solutions. The PGSE NMR attenuation data was measured for bimodal polymer solutions and eq 9 was used to simulate the attenuations via simulations A and B, using the diffusion coefficients measured in the corresponding monomodal polymer solutions. The inclusion of relaxation (see Table 1) into the attenuation equation for these bimodal (50:50 by weight) systems had little or no effect for M_p ratios of 5.4 and 3.4 despite the dependence of the relaxation on the molecular weight. However, in modeling the polymer solution with an M_p ratio of 30.4, the relaxation correction terms are required. Nevertheless, for completeness, the measured relaxation terms were included in all simulations at all three M_p ratios.

The experimentally determined diffusion coefficients for the monomodal PMMA samples, which were subsequently used for simulations A and B, are shown in Figure 2. Also shown are the experimentally determined diffusion coefficients of each component in the bimodal solutions which were found by nonlinear regression of eq 9 onto the data (NB the relaxation terms were fixed to the values in Table 1). Equation 9 was used to avoid unequal weighting to noise as would be the case if the logarithmic form of the equation was used. The experimental diffusion coefficients measured for the components of the bimodal solutions are the weighted averages of the four measurements performed.

The experimental attenuations and simulations for the bimodal systems are shown in Figure 3. Notably nonsingle exponential (i.e., ‘nonlinear’) behavior was found for the sample with an M_p ratio of 30.4 (Figure 3a, if a linear fit was used for the data then an average $R^2 = 0.928 \pm 0.010$ would have been obtained; if the same was done for the data in Figure 3b and c then an average $R^2 = 0.993 \pm 0.002$ and $R^2 = 0.997 \pm 0.001$, respectively, would be obtained). The PGSE

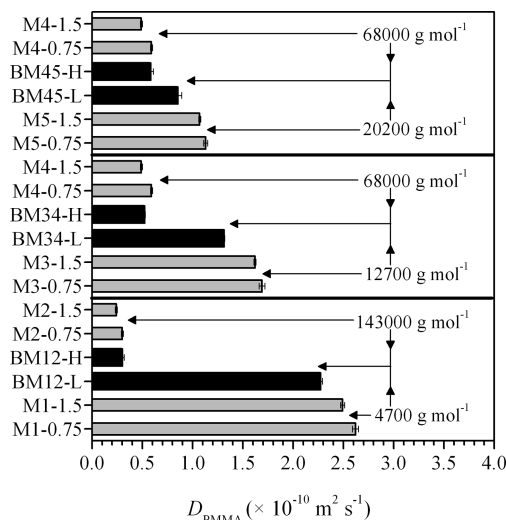


Figure 2. Diffusion coefficients of PMMA: Monomodal solutions (light gray bars (g mol⁻¹); M1 4700; M2 143 000; M3 12 700; M4 68 000; M5 20 200) with concentrations of ~0.75 and ~1.5% w/v. Bimodal solutions (black bars (g mol⁻¹/g mol⁻¹); BM12 4700/143 000; BM34 12 700/68 000; BM45 20200/68 000) where L and H are the results for the low and high M_p components in the bimodal solution, respectively.

NMR attenuations of the bimodal samples with lower M_p ratios (i.e., 3.4 and 5.4) were closely described by simulation A. However, the sample with the highest M_p ratio (i.e., 30.4) was modeled better with simulation B (i.e., the macroscopic average). This difference in behavior could result from obstruction, since the collision frequency will increase as the available space is reduced when the size of one component increases with respect to the other.

However, considering the experimentally determined diffusion coefficients of the components in the bimodal solution obtained when using eq 9, a different situation is evident. The diffusion coefficients of the lowest M_p component in each mixture were affected more than that of the highest M_p component when compared to the diffusion coefficients measured in monomodal solutions (see Figure 2). The diffusion coefficients measured for the highest M_p 's in the mixtures are similar to those measured in a monomodal solution at ~0.75% w/v, but the lowest M_p component of the mixtures are slower than those measured in monomodal solutions even at ~1.5% w/v. The lowest M_p components suffer, as expected, a greater reduction in diffusion coefficient since the hindrance to their motion would be greater. Given these observations a closer look at the simulations for low b values in Figure 3a (see inset) revealed that although simulation B appeared to fit the experimental PGSE NMR attenuation with respect to the full data set, it underestimated it at low b values. At low b values the attenuation was better fitted with simulation A, so in order to better model the experimental PGSE NMR attenuation curves for dilute bimodal solutions of PMMA, it may be necessary to consider a simulation that is a combination of simulations A and B. A simulation where the diffusion coefficient used for the highest M_p was that measured in the monomodal solution at ~0.75% w/v and the diffusion coefficient used for the lowest M_p was that measured in the monomodal solution at ~1.5% w/v was performed and the results are not shown here as the simulated attenuation is very close to that simulated with simulation B with only a subtle, but important, difference at low b values. This new simulation resulted in the data set for an M_p ratio = 30.4 being completely fitted—even at low b values, but the data sets for M_p ratios = 5.4 and 3.4 were still

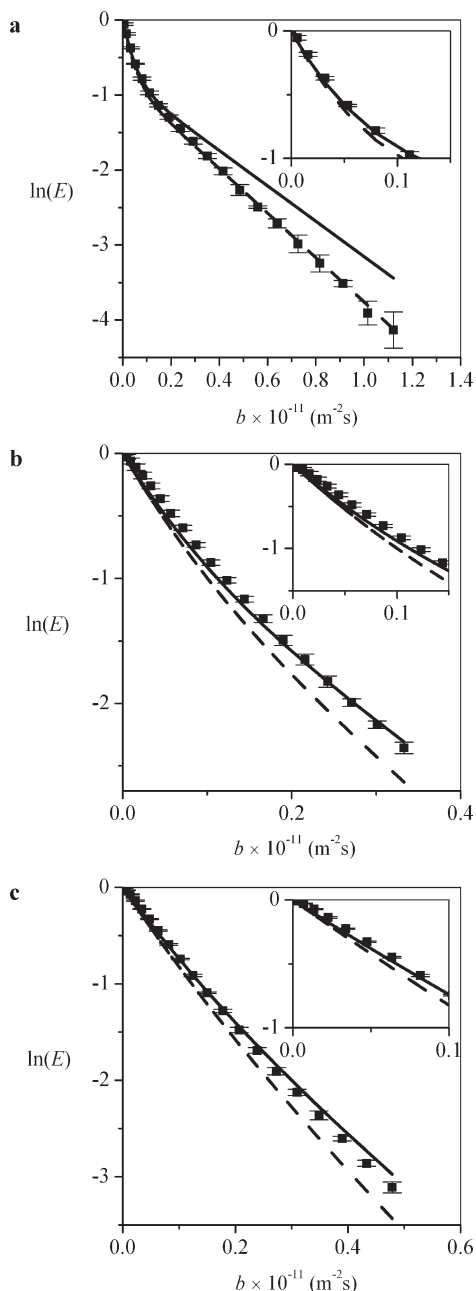


Figure 3. PGSE NMR signal attenuations of bimodal PMMA solutions (M_p ratios: (a) 30.4; (b) 5.4; (c) 3.4) with component polymer concentrations of $\sim 0.75\%$ w/v, giving a total polymer concentration of $\sim 1.5\%$ w/v. Shown are the average experimental data (■) and simulated data using simulation A (—) and simulation B (---). The error bars of the experimental data points are the standard deviation of the four experimental attenuations measured for each bimodal solution. The insets are included to better visualize the fits at low b values.

better fitted by simulation A. The similarity of simulation B and the new simulation is expected as the effect of the higher diffusion coefficient of the lower M_p influences the attenuation greater at low b values.

The results from the biexponential analysis of the bimodal solutions PGSE NMR attenuations suggest obstruction effects are important, particularly for the lowest M_p in the bimodal solution, but as noted earlier, fitting biexponentials is affected by the signal-to-noise ratio, instrumental error, the ratio of the signals of the contributing components, and the ratio of the diffusion coefficients.²⁹ Simulations A and B provided reasonable predictions of the PGSE NMR

attenuations in bimodal solutions. Simulation A described the PGSE NMR attenuation by considering each component to be affected by the increased polymer concentration but expected that the diffusion coefficients were the same as in monomodal solutions of the same total polymer concentration, while simulation B described the PGSE NMR attenuation by considering only macroscopic averaging. When the M_p ratio was highest the attenuation was described by a combination of simulations A and B which corrected the simulation for low b values, but for the two lower M_p ratio solutions the attenuation was still best described by simulation A.

Conclusions

Diffusive averaging behavior is a complicated phenomena and presented in this paper were two simple simulations of PGSE NMR attenuations and their closeness to the experimental attenuations measured for dilute bimodal PMMA solutions. The self-diffusion coefficients used to simulate the attenuations were those from monomodal solutions of the same *total* polymer concentration as the bimodal solution (simulation A) or the self-diffusion coefficients used were those from monomodal solutions of the same *component* concentration as in the bimodal solution (simulation B). The results showed that the macroscopic and microscopic averaging was dependent on the ratio of the molecular weights in the bimodal solution. Simulation A more closely described the attenuation of the dilute bimodal PMMA solutions where the molecular weight difference between the components was small (i.e., M_p ratios = 5.4 and 3.4), and simulation B better described the attenuation of the dilute bimodal PMMA solutions where the molecular weight difference between the components was large (i.e., M_p ratio = 30.4). However, biexponential analysis of the PGSE NMR attenuations suggested that the diffusion coefficient of the highest M_p was similar to that measured in the monomodal solutions of the same *component* concentration, but the lowest M_p components diffusion coefficient was much slower than even measured in monomodal solutions of the same *total* polymer concentration. A simulation based on a combination of simulations A and B where the self-diffusion coefficients used to simulate the attenuation was those from monomodal solutions of the same *total* polymer concentration for the lowest M_p and the same *component* concentration for the highest M_p as the bimodal solution was performed. This simulation resulted in the experimental attenuation being better described only for the solution of the highest M_p ratio.

Acknowledgment. This research was supported by a University of Western Sydney Honours Scholarship (S.A.W.) and a NSW BioFirst Award from the NSW Ministry for Science & Medical Research (W.S.P.).

References and Notes

- (1) Crank, J., *Mathematics of Diffusion*. 2nd ed.; Oxford University Press: New York, 1975.
- (2) Price, W. S. *Concepts Magn. Res.* **1997**, *9*, 299–336.
- (3) Price, W. S. *Annu. Rep. Prog. Chem., Sect. C* **2000**, *96*, 3–53.
- (4) Sutherland, W. *Philos. Mag.* **1905**, *9*, 781–785.
- (5) Bringuier, E.; Bourdon, A. *Physica A* **2007**, *385*, 9–24.
- (6) Therien-Aubin, H.; Zhu, X. X.; Moorefield, C. N.; Kotta, K.; Newkome, G. R. *Macromolecules* **2007**, *40*, 3644–3649.
- (7) Price, W. S. *Curr. Opin. Colloid Interface Sci.* **2006**, *11*, 19–23.
- (8) Price, W. S. *NMR Studies of Translational Motion*. Cambridge University Press: New York, 2009.
- (9) Nilsson, M.; Hakansson, B.; Söderman, O.; Topgaard, D. *Macromolecules* **2007**, *40*, 8250–8258.
- (10) Callaghan, P. T.; Pinder, D. N. *Macromolecules* **1985**, *18*, 373–379.
- (11) Stejskal, E. O.; Tanner, J. E. *J. Chem. Phys.* **1965**, *42*, 288–292.
- (12) Price, W. S. *Concepts Magn. Res.* **1998**, *10*, 197–237.

- (13) Price, W. S.; Stilbs, P.; Jonsson, B.; Söderman, O. *J. Magn. Reson.* **2001**, *150*, 49–56.
- (14) Price, W. S.; Wälchli, M. *Magn. Reson. Chem.* **2002**, *40*, S128–S132.
- (15) Johnson, C. S., Jr. *Prog. Nucl. Mag. Res. Sp.* **1999**, *34*, 203–256.
- (16) Han, J.; Herzfeld, J. *Biophys. J.* **1993**, *65*, 1155–1161.
- (17) Price, W. S.; Tsuchiya, F.; Arata, Y. *J. Am. Chem. Soc.* **1999**, *121*, 11503–11512.
- (18) Inglis, S. R.; McGann, M. J.; Price, W. S.; Harding, M. M. *FEBS Lett.* **2006**, *580*, 3911–3915.
- (19) Fleischer, G. *Polymer* **1985**, *26*, 1677–1682.
- (20) Callaghan, P. T.; Pinder, D. N. *Macromolecules* **1983**, *16*, 968–973.
- (21) Raghavan, R.; Maver, T. L.; Blum, F. D. *Macromolecules* **1987**, *20*, 814–818.
- (22) Cosgrove, T.; Griffiths, P. C. *Polymer* **1995**, *36*, 3335–3342.
- (23) Cosgrove, T.; Griffiths, P. C. *Polymer* **1995**, *36*, 3343–3347.
- (24) von Meerwall, E. D. *J. Magn. Reson.* **1982**, *50*, 409–416.
- (25) Vancso, G. *Eur. Polym. J.* **1990**, *26*, 345–348.
- (26) White, B. R.; Vancso, G. J. *Eur. Polym. J.* **1992**, *28*, 699–702.
- (27) Koppel, D. E. *J. Chem. Phys.* **1972**, *57*, 4814–4820.
- (28) Kubo, R. *J. Phys. Soc. Jpn.* **1962**, *17*, 1100.
- (29) Nilsson, M.; Connell, M. A.; Davis, A. L.; Morris, G. A. *Anal. Chem.* **2006**, *78*, 3040–3045.
- (30) Jerschow, A.; Müller, N. *Macromolecules* **1998**, *31*, 6573–6578.
- (31) Price, W. S.; Tsuchiya, F.; Arata, Y. *Biophys. J.* **2001**, *80*, 1585–1590.
- (32) Cavanagh, J.; Fairbrother, W. J.; Palmer III, A. G.; Rance, M.; Skelton, N. J. *Experimental Aspects of Nmr Spectroscopy*. In *Protein NMR Spectroscopy*, 2nd ed.; Academic Press: Burlington, NJ, 2007; pp 114–270.
- (33) Raiford, D. S.; Fisk, C. L.; Becker, E. D. *Anal. Chem.* **1979**, *51*, 2050–2051.
- (34) Jerschow, A.; Müller, N. *J. Magn. Reson.* **1997**, *125*, 372–375.
- (35) Chen, A.; Johnson, C. S.; Lin, M.; Shapiro, M. J. *J. Am. Chem. Soc.* **1998**, *120*, 9094–9095.
- (36) Levitt, M., H., *Spin Dynamics—Basics of Nuclear Magnetic Resonance*; John Wiley & Sons, Ltd.: Chichester, U.K., 2001.
- (37) Vold, R. L.; Waugh, J. S.; Klein, M. P.; Phelps, D. E. *J. Chem. Phys.* **1968**, *48*, 3831–3832.
- (38) Carr, H. Y.; Purcell, E. M. *Phys. Rev.* **1954**, *94*, 630–638.
- (39) Meiboom, S.; Gill, D. *Rev. Sci. Instrum.* **1958**, *29*, 688–691.
- (40) Sagidullin, A.; Fritzing, B.; Scheler, U.; Skirda, V. D. *Polymer* **2004**, *45*, 165–170.
- (41) Sagidullin, A. I.; Muzafarov, A. M.; Krykin, M. A.; Ozerin, A. N.; Skirda, V. D.; Ignat'eva, G. M. *Macromolecules* **2002**, *35*, 9472–9479.